Preprints of the 21st IFAC World Congress (Virtual)
Berlin, Germany, July 12-17, 2020

Dynamic Modelling of Obstetric Patient Coagulation from Kaolin-Activated Thromboelastogram Data ⋆

Kieran P. Fitzmaurice * **Michelle A. Pressly** *
Gilles Clermont **,* **Jonathan H. Waters** ***,****
Robert S. Parker *,**,****

* *Department of Chemical and Petroleum Engineering, University of Pittsburgh, Pittsburgh, PA 15261 USA (e-mail: kpf10@pitt.edu, map312@pitt.edu, rparker@pitt.edu).*
** *Department of Critical Care Medicine, University of Pittsburgh, Pittsburgh, PA 15261 USA (e-mail: cler@pitt.edu)*
*** *Department of Anesthesiology, University of Pittsburgh, Pittsburgh, PA 15261 USA (e-mail: watejh@upmc.edu)*
**** *Department of Bioengineering, University of Pittsburgh, Pittsburgh, PA 15261 USA*

Abstract: Defects in blood clotting (coagulopathies) are linked to severe outcomes in mothers suffering from obstetrical hemorrhage. Identifying patients with a coagulopathy poses a challenge for clinicians, who are required to make quick treatment decisions in fast-paced environments with a high degree of uncertainty. Integrating data from point-of-care coagulation tests with mathematical models of coagulation presents an exciting opportunity to improve patient outcomes by reducing this uncertainty. A model with parameters estimated from individual patient data can provide clinicians with a way to compare patients and group them into categories of probable coagulopathy based on biologically-interpretable parameters. With this in mind, we developed a mechanism-inspired model of blood coagulation calibrated against thromboelastogram (TEG) data. Markov Chain Monte Carlo and sensitivity analysis were used to assess the identifiability and distribution of model parameters for 25 obstetric patients. The ability of our model to separate patients in parameter space based on differences in observed TEG response lends credence to the feasibility of using dynamic models as tools for identifying coagulopathy subtypes within the obstetric population.

Keywords: Nonlinear Dynamic Modelling, Coagulation, Thromboelastography, Obstetrics, Systems Medicine, Markov Chain Monte Carlo.

1. INTRODUCTION

Obstetrical hemorrhage is a leading cause of maternal mortality in the United States, accounting for 16.2% of all pregnancy-related deaths between 2003 and 2011 (Kuriya et al. (2016)). Risk factors associated with this condition include advanced maternal age, placental complications during pregnancy, and the presence of postpartum coagulopathy. Coagulopathies are a class of bleeding disorders characterized by deficits or defects in the coagulation system that result in an impaired ability to form or maintain blood clots. Severe post-delivery bleeding often requires serious interventions such as uterotonic agents, massive transfusion, or hysterectomy surgery (Butwick and Goodnough (2015)); therefore, determining whether a mother has an abnormally weak clotting ability at or before the onset of bleeding is a critical factor in selecting the correct level and type of treatment needed to prevent dangerous amounts of blood loss. However, in practice these patients are often identified only after they fail to respond to standard treatments. Because of patient-to-patient variability associated with coagulation, there exists a strategic need to improve outcomes through the implementation of tools that enable clinicians to compare patients and group them by severity and subtype of coagulopathy.

A point-of-care device commonly used to assess the presence and degree of coagulopathy is the thromboelastogram (TEG). This device oscillates a sample of whole blood mixed with a reagent (typically kaolin or tissue factor) to activate coagulation, which is measured via the displacement of a small pin (Hae (2014)). By recording the amplitude (in mm) of these oscillations over time, the device outputs a quantitative representation of clot formation and subsequent breakdown (clot lysis). TEG parameters describing the shape of this response provide physicians with patient-specific measures of

⋆ Financial support for this work is provided by the National Science Foundation's TECBio REU program (DBI-1659611), the U.S. Department of Education GAANN fellowship program (P200A150050), and the National Institutes of Health, National Heart, Lung and Blood Institute (R21-HL-133891).

clotting ability, which guide treatment protocols in areas such as trauma and obstetrics (Karlsson et al. (2014)). Commonly used parameters include the latent time between the start of the test and first recorded displacements of the pin (R-time), the maximum recorded amplitude of displacements (MA), and the percentage decrease in amplitude 30 minutes after MA is reached (LY30).

Current thromboelastogram parameters characterize TEG tracings using macroscopic measurements taken at discrete points in time. However, a more complete way to describe these curves is to use ordinary differential equations (ODEs), which provide a flexible and accurate way of explaining how the variety of observed TEG response shapes all arise from a common, dynamic process. TEG tracings of individual patients may be precisely specified by a set of ODE model parameters estimated from measured data. By examining the distribution of model parameters across patient populations, specific regions of parameter space can be tied to specific breakdowns of the coagulation system, thereby enabling individualized coagulation assessment and subsequent treatment.

Mathematical modelling has yet to be widely implemented in the context of coagulation management in a clinical setting; however, in recent years there has been renewed interest in incorporating knowledge of coagulation dynamics into resuscitation protocols. Menezes et al. (2017) outlined a methodology for rectifying coagulation deficits in trauma patients that uses systems identification techniques to model the effect that additions of key clotting factors will have on thrombin generation *in vitro*. Mechanism-inspired dynamic models could also be used to this end, and carry the added benefit of having states and parameters which are more easily related to the underlying biological process. Existing mechanistic models typically feature a large number of states and parameters (76 biochemical species and 105 kinetic constants in the case of a systems biology model developed by Chatterjee et al. (2010)). The complexity of these models hinders their application to obstetric medicine; fitting such a large number of parameters on a per-patient basis would require an amount and quality of data beyond what is available in a clinical environment. Thus, there is a need for simpler, low-order models that strike a balance between physiologic realism and clinical utility. With this in mind, our model is designed to provide insight into the dynamics of several key clot components in a reduced-order framework, and is calibrated using patient TEG data.

2. METHODS

2.1 Thromboelastogram Data

Data from 108 kaolin TEGs run on a TEG 5000 Hemostasis Analyzer System (Hae (2014)) were collected from UPMC Magee-Womens Hospital in Pittsburgh, PA. Of the full set of 108 collected TEGs, only 58 TEGs (from 25 unique patients) were identified from the obstetric population. After taking the earliest available TEG for each patient, a final sample of n=25 TEGs were analyzed with our computational methods.

2.2 Model Structure

The kaolin TEG response model was built using mass conservation principles and consists of a simplified reaction scheme that describes the dynamics of several clinically-relevant species in coagulation. Rather than describing the true biochemical reactions at work, the kinetic rate equations in our model represent low-order approximations of the major interactions that occur between different components. The resulting dynamic model, while mechanism-inspired, is an analogy for (rather than an explicit representation of) the underlying biology. The advantage of this approach is that the parameters of a simple model are more likely to be identifiable from individual TEG tracings.

Our model describes coagulation as occurring through the following simplified reaction scheme. An addition of kaolin triggers the conversion of prothrombin to its active form, thrombin, at a small initial rate (1). The resulting interaction of thrombin with resting platelets causes the latter to activate (2). Activated platelets provide sites for surface-mediated reactions that rapidly convert prothrombin to thrombin, generating large amounts of the latter (3). Thrombin then reacts with fibrinogen to form a cross-linked fibrin network, which, together with aggregated platelets, results in a clot (4). This clot is subsequently broken down via fibrinolysis (5).

$$pT \xrightarrow{k_1} T \tag{1}$$

$$P + T \xrightarrow{k_2} P_a + T \tag{2}$$

$$P_a + pT \xrightarrow{k_3} P_a + T \tag{3}$$

$$P_a + T + Fg \xrightarrow{k_4} C \tag{4}$$

$$C \xrightarrow{k_5} \varnothing \tag{5}$$

In order to capture intermediate states of platelet activation, the activation process depicted in (2) was split up into three stages. Discretizing this step in our reaction scheme proved useful for capturing patients with longer R-times. The network that results from this description of coagulation is depicted in Fig.1.

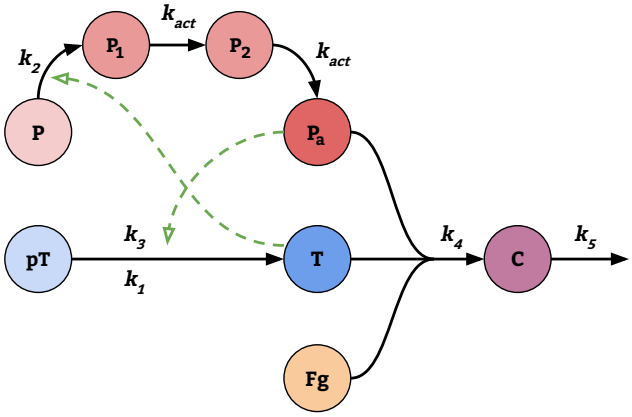

Fig. 1. Simplified description of coagulation: solid arrows indicate generation or consumption of different species in our model, while dashed arrows indicate activating or catalytic interactions.

By approximating the TEG as a well-mixed vessel, reaction kinetics may be represented as a system of ODEs. Our system consists of the following states corresponding to species concentrations: prothrombin, $pT(t)$, thrombin, $T(t)$, resting platelets, $P(t)$, intermediate activation states, $P_1(t)$ and $P_2(t)$, fully activated platelets, $P_a(t)$, fibrinogen, $Fg(t)$, as well as the clot state, $C(t)$.

$$\frac{dpT(t)}{dt} = -k_1 pT(t) - k_3 P_a(t) \cdot \frac{pT(t)}{\mu_{pT} + pT(t)} \tag{6}$$

$$\frac{dT(t)}{dt} = k_1 pT(t) + k_3 P_a(t) \cdot \frac{pT(t)}{\mu_{pT} + pT(t)} - k_4 T(t) \cdot \frac{P_a(t)}{\mu_{P_a} + P_a(t)} \cdot \frac{Fg(t)}{\mu_{Fg} + Fg(t)} \tag{7}$$

$$\frac{dP(t)}{dt} = -k_2 P(t) \cdot \frac{T(t)}{\mu_T + T(t)} \tag{8}$$

$$\frac{dP_1(t)}{dt} = k_2 P(t) \cdot \frac{T(t)}{\mu_T + T(t)} - k_{act} P_1(t) \tag{9}$$

$$\frac{dP_2(t)}{dt} = k_{act} P_1(t) - k_{act} P_2(t) \tag{10}$$

$$\frac{dP_a(t)}{dt} = k_{act} P_2(t) - k_4 T(t) \cdot \frac{P_a(t)}{\mu_{P_a} + P_a(t)} \cdot \frac{Fg(t)}{\mu_{Fg} + Fg(t)} \tag{11}$$

$$\frac{dFg(t)}{dt} = -k_4 T(t) \cdot \frac{P_a(t)}{\mu_{P_a} + P_a(t)} \cdot \frac{Fg(t)}{\mu_{Fg} + Fg(t)} \tag{12}$$

$$\frac{dC(t)}{dt} = k_4 T(t) \cdot \frac{P_a(t)}{\mu_{P_a} + P_a(t)} \cdot \frac{Fg(t)}{\mu_{Fg} + Fg(t)} - k_5 C(t) \tag{13}$$

Equations (6)-(13) describe an abstracted representation of coagulation biology, but one that nevertheless incorporates many essential features of the underlying system. The resulting system of ODEs is parameterized by 6 rate coefficients (k_1, k_2, k_3, k_4, k_5, k_{act}), 4 saturation constants (μ_{pT}, μ_T, μ_{P_a}, μ_{Fg}), and 8 initial concentrations (one for each state). To relate our model to experimental data, the clot state $C(t)$ is scaled to patient TEG data via a scaling factor ψ–itself an estimated parameter with units of mm.

$$y(t) = \psi \cdot C(t) \tag{14}$$

2.3 Bayesian Parameter Estimation

Parameter estimation was accomplished using APT-MCMC (Zhang et al. (2018)), a C++/Python implementation of a Markov Chain Monte Carlo algorithm with parallel tempering. MCMC is a stochastic technique used to gain information about probability distributions lacking a closed form, in which random "walkers" generate samples of the parameter space according to the probability of a given parameter set in the face of observed experimental data. This process is enhanced by parallel tempering, a physics-based method in which information exchange between Markov chains run in parallel at different "temperatures" enables both a broad and deep search of parameter space. From a large number of samples, MCMC recovers the posterior distribution of model parameters, which may be used to develop confidence intervals, assess interparameter correlations, and identify the locations of multiple minima in the objective function surface. In our analysis, the maximum likelihood parameter vector and confidence intervals for each patient were calculated via kernel density estimation using the last 10,000 parameter vectors returned by APT-MCMC out of a total chain of 100,000.

2.4 Sensitivity Analysis

By computing the sensitivity matrix around nominal parameter values returned from APT-MCMC, it is possible to determine which parameters have the most influence on the measured variable $y(t)$. As demonstrated by Zak et al. (2003), parametric sensitivity is also related to identifiability, to the extent that parameters whose sensitivities are highly correlated can influence the measured variable in a compensatory manner to one another–thus forming an unidentifiable group. In our analysis, sensitivities were used to evaluate the relative importance and identifiability of model parameters.

2.5 Identifiability Analysis and Model Reduction

In the context of nonlinear ODE systems, MCMC becomes a powerful tool for assessing model robustness and the identifiability of parameters from available data. Insufficient or sparse data often results in excessively large confidence intervals on estimated parameters; mitigating this issue typically requires reducing the number of free parameters in the model. With this in mind, APT-MCMC and sensitivity analysis were used to guide the reduction of our original set of parameters to a subset that may be uniquely estimated from patient TEG tracings.

The coupled processes of platelet activation and thrombin generation form a powerful positive feedback loop, which in our model is driven by the rate coefficients k_1, k_2, k_3 and k_{act}. Analysis of the sensitivity matrices for 25 patients indicated that these four parameters have a highly correlated effect on $y(t)$, suggesting that they are unidentifiable from TEG data alone. This group was reduced to an identifiable subset by fixing k_1 and k_{act} at constant values, and setting k_2 and k_3 in equations (6)-(9) as being equal to single estimated value, henceforth referred to as β. In addition, the confidence intervals on saturation constants indicated that they were not adequately estimable from TEG data; therefore, all values of μ in equations (6)-(13) were set to a fixed value of 0.5. In the reduced formulation of our model, all states are scaled to have initial values of either 0 or 1, indicating concentration at the onset of coagulation in arbitrary units.

After model reduction, our final structure includes four estimated parameters: the rate coefficient governing platelet activation and thrombin generation (β), the rate coefficients of clot formation (k_4) and lysis (k_5), as well as the scaling factor ψ. In order to ensure that the $P_a(t)$ state is distinguishable, it is necessary to set the upper bound of k_4 to a value within an order of magnitude of k_{act}. Considered ranges of estimated parameters and values of fixed constants are detailed in Table 1 and Table 2.

Table 1. Estimated Parameters

Parameter	Range	Units	Description
β	[0.0001, 1]	s^{-1}	Resting platelet activation and thrombin generation rate constant (value of k_2 and k_3)
k_4	[0.0001, 0.1]	s^{-1}	Clot formation rate constant
k_5	$[1 \times 10^{-7}, 0.001]$	s^{-1}	Clot lysis rate constant
ψ	[0, 70]	mm	Scaling factor between clot state and TEG readout

Table 2. Fixed Parameters and Initial Conditions

Parameter	Value	Units	Description
k_1	1×10^{-6}	s^{-1}	Rate constant of thrombin generation from kaolin reagent
k_{act}	0.01	s^{-1}	Platelet transformation rate
μ_{pT}, μ_T, μ_{P_a}, μ_{Fg}	0.5	arb.	Saturation constants
$pT(0)$, $P(0)$, $Fg(0)$	1	arb.	Initial concentration of species present at onset of coagulation
$T(0)$, $P_1(0)$, $P_2(0)$, $P_a(0)$, $C(0)$	0	arb.	Initial concentration of species absent at onset of coagulation

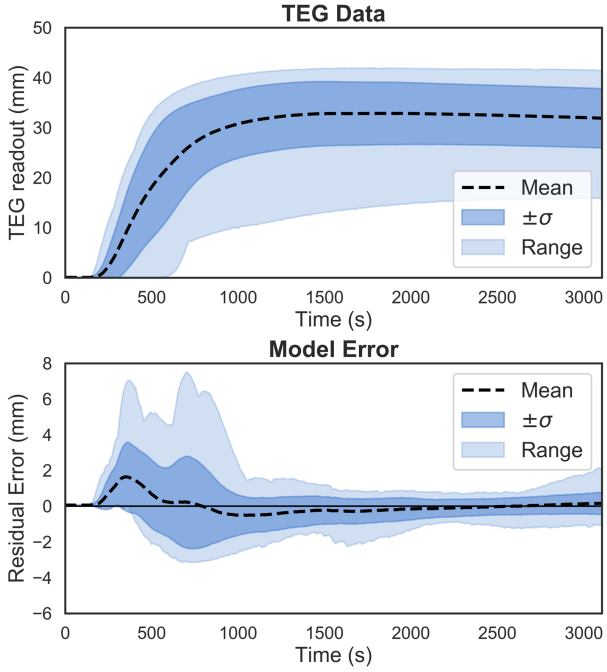

Fig. 2. TEG data and model error: the mean, standard deviation, and range of experimental values (top) and model error (bottom) at each time point for all 25 patients. Residual error is defined as actual TEG value (in mm) at each time point minus that predicted by the model.

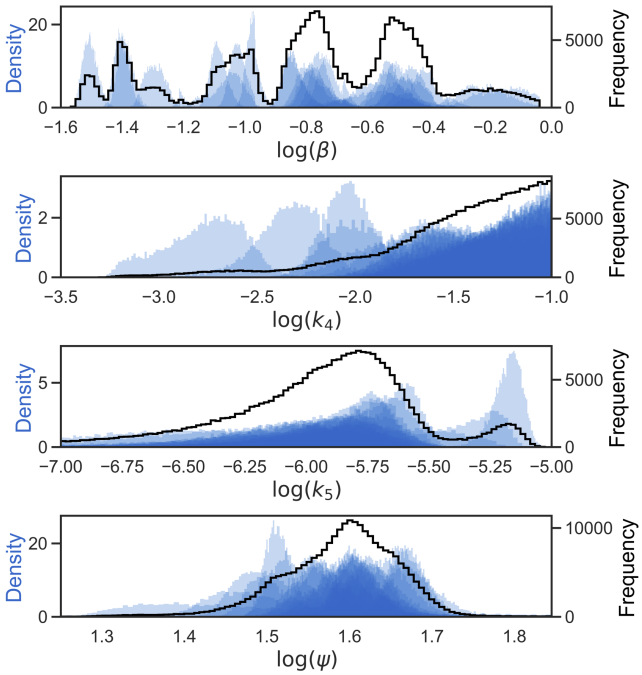

Fig. 3. Model Parameters: The last 10,000 parameter vectors output by APT-MCMC fits for each individual TEG were normalized to produce the distributions shown in blue (left y-axis), and the overall frequencies across all 25 patients added together to produce the population histograms shown in black (right y-axis).

3. RESULTS

The model predicted TEG tracings corresponding to the maximum likelihood parameter vector for each patient result in an average absolute error of 0.62 mm at each time point. Plots of the mean residual error at each time point, as well as the standard deviation and range across the data set, are shown in Fig. 2. The model exhibits an ability to capture TEG tracings with a high degree of accuracy, especially towards the later portions of the readout in which the clot has ceased growing and begins to undergo the process of lysis.

The majority of error occurs during the period of rapid clot growth, a process primarily governed by k_4, which controls the rate of platelet aggregation and fibrin polymerization. Our model underpredicts the rate of clot growth, which we attribute to the model structure compensating for decidedly variable R-times observed within our data set, as well as the bounds set on k_4. Although some of this error could likely be reduced by relaxing the allowed range of k_4 (Table 1), these limits were deliberately introduced to restrict the dynamic range of $P_a(t)$ such that activated platelets have time to accumulate to appreciable levels before they are incorporated into the clot.

3.1 Population Histograms

APT-MCMC fits to TEGs from all 25 patients are displayed in Fig. 3. By examining how the distributions of β, k_4, k_5, and ψ vary across our data set, it becomes evident how specific shapes seen in TEG tracings are linked to the values of estimated model parameters.

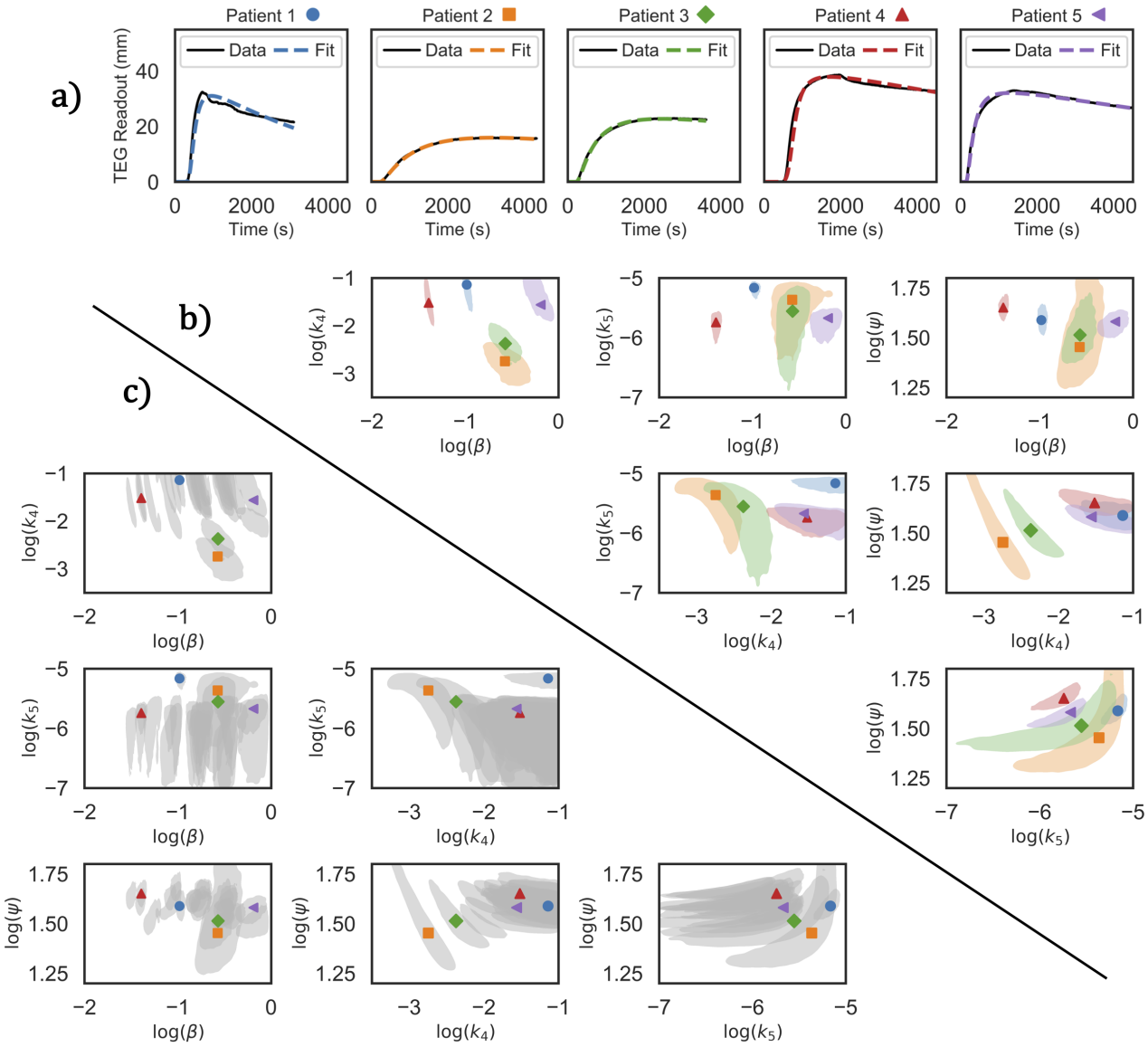

Fig. 4. Patient Subtypes: (a) Model fits to TEG data for 5 different patients from the 25 patient population. (b) Joint probability distributions of parameters fit to selected patients. (c) Joint probability distributions for all 25 patients superimposed. The locations of the maximum likelihood parameter sets used to generate the fits in (a) are indicated by markers in (b) and (c), with 95% confidence regions for each patient shown as shaded areas in panel (b).

The time between the addition of the kaolin reagent and first recorded oscillations of the pin (R-time) can vary greatly between patients; this manifests as multimodalities the distribution of β, which controls the aggressiveness of the positive feedback loop formed by platelet activation and thrombin generation. This suggests there exists significant interpatient differences in coagulation initiation across the population and that these differences may contribute to the identification of distinct subpopulations. The majority of TEG tracings examined exhibit a rapid rate of clot growth in the minutes after R-time is achieved, resulting in k_4 distributions that are shifted towards the parameter's upper bound. However, there exists a small but clinically relevant group of patients inhabiting the left half of the k_4 range; for these patients, clot growth occurs at a much slower rate, suggesting an impaired ability to generate clot-forming species such as activated platelets and fibrin. Most TEGs exhibit a low rate of clot lysis, with the exception of two patients whose high lysis rates place their k_5 distributions distinctly to the right of the overall population. The scaling factor ψ is related to the magnitude of TEG response produced by a patient's clot–a measurement that serves as a proxy for clot size and strength. In our patient population, distributions of ψ tend to overlap and are clustered around a value of approximately 40 mm.

3.2 Subtyping in Parameter Space

The marginal distributions of fitted parameters returned by APT-MCMC can be combined into joint distribution plots to provide a two-dimensional visualization of the model parameter space (Fig. 4). At the population level, this provides a means for exploring how differences in patient coagulopathic state (as measured by TEG data) manifest as separation in the model parameter space.

Figs. 4a and 4b illustrate how different coordinates in parameter space define TEG response dynamics for several patient subtypes observed within our data set. Model fits to TEG data for five patients are shown in Fig. 4a. The high lysis subtype (Patient 1), exhibits a high degree of separation from the overall population along the $\log(k_5)$ axis. Patients that fall under the slow clot growth subtype (Patients 2 and 3) are distinguished by their outlying position along the $\log(k_4)$ and $\log(\psi)$ axes. Joint distribution plots for Patients 2 and 3 indicate the existence of a linear correlation between $\log(k_4)$ and $\log(\psi)$ not found in the majority of patients (Pearson correlation coefficient of -0.97 and -0.92 for Patients 2 and 3 respectively, compared to a mean value of -0.64 for all 25 patients). This can be attributed to the fact that TEGs for the slow clot growth subtype in our data set typically do not have time to capture the process of clot lysis before the test is terminated, making it difficult to quantify k_5 and separate the relative contributions of k_4 and ψ to the measured response. This is further evidenced by the presence of a slight nonlinear correlation seen between $\log(k_5)$ and $\log(\psi)$ for this patient type. Patients 4 and 5 represent the long and short R-time subtypes respectively, but otherwise feature TEG tracings typical of the majority of patients in the data set. In the model parameter space, they are clustered closely together except when plotted along the $\log(\beta)$ axis.

4. SUMMARY

From a data set of 25 kaolin-activated TEGs taken from the obstetric population, a dynamic model of coagulation was constructed. An identifiability analysis, guided by APT-MCMC and further validated by sensitivity analysis, led to the reduction of model parameter space to four parameters shown to be estimable from TEG data. The resulting model exhibited an ability to fit different types of TEG tracings encountered in the clinic, with interpatient differences in clotting ability (as measured by TEG response shape) leading to separation when plotted in the model parameter space–thus demonstrating the plausibility of using model parameters to identify subtypes of coagulopathy.

The mechanism-inspired nature of our model structure could enable the linking of locations in parameter space to specific impairments of the coagulation cascade. With this context in mind, dynamic modelling can help clinicians not only detect the presence of coagulopathy, but potentially pinpoint where the breakdown is occurring in the underlying biological system, which informs the subsequent choice of treatment.

A major barrier to the implementation of model-based coagulation control is the difficulty of incorporating thromboelastogram data into a decision support system in real time. Ideally, such a system would be part of a point-of-care platform that integrates TEG data with a dynamic model, thus providing clinicians with up-to-the-minute assessments of potential breakdowns in the coagulation process while the TEG is run. Given that commercially-available TEGs have the capability to display results in real time to a hospital workstation via their manufacturers' viewing interface, integration of this type of assessment would only require additions to existing software.

We are in the process of accessing and fitting additional obstetric patients to evaluate the robustness of identified subtypes, as well as evaluating how patient subtype may change over time or as the result of clinical intervention. In addition, incorporating data from other point-of-care tests of hemostasis (e.g., thrombin generation assay, platelet count, fibrinogen Clauss assay, etc.), may enable the mapping of internal model states to physiologic quantities, providing clinicians with actionable data on what modes of intervention may be used to return patients to a healthy overall coagulation state.

ACKNOWLEDGEMENTS

Financial support for this work is provided by the TECBio REU @ Pitt program supported by the National Science Foundation (DBI-1659611), the U.S. Department of Education Graduate Assistance in Areas of National Need fellowship program (P200A150050), and the National Institutes of Health, National Heart, Lung and Blood Institute (R21-HL-133891). The authors declare no conflict of interest.

REFERENCES

(2014). *TEG 5000 Hemostasis Analyzer System*. Haemonetics. URL `https://teg.haemonetics.com/`. TEG 5000 educational brochure.

Butwick, A.J. and Goodnough, L.T. (2015). Transfusion and coagulation management in major obstetric hemorrhage. *Current Opinion in Anesthesiology*, 28(3), 275–284.

Chatterjee, M.S., Denney, W.S., Jing, H., and Diamond, S.L. (2010). Systems biology of coagulation initiation: kinetics of thrombin generation in resting and activated human blood. *PLoS Computational Biology*, 6(9), e1000950.

Karlsson, O., Jeppsson, A., and Hellgren, M. (2014). Major obstetric haemorrhage: monitoring with thromboelastography, laboratory analyses or both? *International Journal of Obstetric Anesthesia*, 23(1), 10–17.

Kuriya, A., Piedimonte, S., Spence, A., Czuzoj-Shulman, N., Kezouh, A., and Abenhaim, H.A. (2016). Incidence and causes of maternal mortality in the USA. *Journal of Obstetrics and Gynaecology Research*, 42(6), 661–668.

Menezes, A.A., Vilardi, R.F., Arkin, A.P., and Cohen, M.J. (2017). Targeted clinical control of trauma patient coagulation through a thrombin dynamics model. *Science Translational Medicine*, 9(371), eaaf5045.

Zak, D.E., Gonye, G.E., Schwaber, J.S., and Doyle, F.J. (2003). Importance of input perturbations and stochastic gene expression in the reverse engineering of genetic regulatory networks: insights from an identifiability analysis of an in silico network. *Genome Research*, 13(11), 2396–2405.

Zhang, L.A., Urbano, A., Clermont, G., Swigon, D., Banerjee, I., and Parker, R.S. (2018). APT-MCMC, a C++/Python implementation of Markov Chain Monte Carlo for parameter identification. *Computers & Chemical Engineering*, 110, 1–12.